


## Quasibound state in the $\bar{K}NNN$ system

N. V. Shevchenko <sup>\*</sup>

Nuclear Physics Institute, 25068 Řež, Czech Republic



(Received 29 June 2022; accepted 7 October 2022; published 27 December 2022)

The paper is devoted to the  $\bar{K}NNN$  system, which is an exotic system consisting of an antikaon and three nucleons. Dynamically exact four-body Faddeev-type equations were solved, and characteristics of the quasibound state in the  $K^-ppn$  system caused by strong interactions were evaluated. Three antikaon-nucleon and three nucleon-nucleon potentials were used, so the dependence of the four-body pole positions on the two-body interaction models was studied. The resulting binding energies  $B_{K^-ppn}^{\text{Chiral}} \approx 30.5\text{--}34.5$  MeV obtained with the chirally motivated and  $B_{K^-ppn}^{\text{SIDD}} \approx 46.4\text{--}52.0$  MeV obtained with the phenomenological antikaon-nucleon potentials are close to those obtained for the  $K^-pp$  system with the same  $\bar{K}N$  and  $NN$  potentials, while the four-body widths  $\Gamma_{K^-ppn} \approx 38.2\text{--}50.9$  MeV are smaller.

DOI: [10.1103/PhysRevC.106.064006](https://doi.org/10.1103/PhysRevC.106.064006)

### I. INTRODUCTION

The attractive nature of  $\bar{K}N$  interaction leads to suggestions that quasibound states can exist in few-body systems consisting of antikaons and nucleons [1]. In particular, a deep and relatively narrow quasibound state was predicted in the lightest three-body  $\bar{K}NN$  system [2]. Many theoretical calculations of the system were performed after that using different methods and inputs. All of them agree, that the quasibound state exists in the spin-zero state of  $\bar{K}NN$ , usually denoted as  $K^-pp$ , but predict quite different binding energies and widths of the state.

The experimental situation is unsettled as well: several candidates for the  $K^-pp$  state were reported by different experiments [3–5], while other experiments left the matter unsettled [6,7]. However, the measured binding energies and especially decay widths of the state differ from each other and are far from all theoretical predictions. The most recent results by the J-PARK E15 experiment [8,9] for the binding energy are comparable to some theoretical predictions, but the corresponding width of the  $K^-pp$  quasibound state is much larger.

In recent years we performed a series of calculations of different states of the three-body  $\bar{K}NN$  and  $\bar{K}\bar{K}N$  systems, described in Ref. [10], using dynamically exact Faddeev-type equations in Alt-Grassberger-Sandhas form with coupled  $\bar{K}NN$  and  $\pi\Sigma N$  channels. In particular, we evaluated  $K^-pp$  quasibound state binding energy and width using three different models of  $\bar{K}N$  interaction. The same was done for the  $\bar{K}\bar{K}N$  system. We also demonstrated that there is no quasibound state, caused by pure strong interactions, in spin-one state of  $\bar{K}NN$  system, which is  $K^-np$ . In addition, we cal-

culated near-threshold amplitudes of  $K^-$  elastic scattering on deuterons. Finally, we evaluated the  $1s$  level shift in kaonic deuterium, which is an atomic state, caused by the presence of the strong  $\bar{K}N$  interaction in comparison to the pure Coulomb state.

The four-body  $\bar{K}NNN$  system is another system with strangeness which could shed more light on the question of antikaon-nucleon interaction. Kaonic helium, an atomic state caused mainly by the Coulomb interaction, was studied in several experiments. The most recent one was performed by the J-PARK E62 Collaboration, see Ref. [11] and references therein. Theoretical investigation of the four-body kaonic atom is complicated due to necessity to describe long-range Coulomb and short-range strong interactions simultaneously.

Several experimental searches of the quasibound state in the  $\bar{K}NNN$  system caused by the strong interactions were performed without conclusive results. A peak structure below the  $K^- + p + p + n$  threshold was recently observed in J-PARK T77 data [12], which was interpreted as a possible signal of the “strong”  $\bar{K}NNN$  quasibound state. Experimental investigation of the  $\bar{K}NNN$  state, similar to the quasibound state in the  $K^-pp$  system, is planned in a J-PARK E80 experiment [12].

Some theoretical calculations of the quasibound state in the  $\bar{K}NNN$  system caused by strong interactions were already performed [1,13–15], but more accurate calculations are needed. Binding energy and width of the state were calculated in the present study using four-body Faddeev-type equations by Grassberger and Sandhas [16]. Only these dynamically exact equations in momentum representation can treat exactly the energy-dependent  $\bar{K}N$  potentials necessary for this system. Our two-body antikaon-nucleon interaction models, constructed for the three-body Faddeev calculations [10], were used as input.

<sup>\*</sup>shevchenko@ujf.cas.cz

## II. FOUR-BODY FADDEEV-TYPE EQUATIONS

The three-body Faddeev-type equations in Alt-Grassberger-Sandhas (AGS) form [17],

$$U_{\alpha\beta}(z) = (1 - \delta_{\alpha\beta})G_0^{-1}(z) + \sum_{\gamma=1}^3 (1 - \delta_{\alpha\gamma})T_\gamma(z)G_0(z)U_{\gamma\beta}(z), \quad (1)$$

define the three-body transition operators  $U_{\alpha\beta}(z)$ , which describe the process  $\beta + (\alpha\gamma) \rightarrow \alpha + (\beta\gamma)$ . The  $G_0(z)$  in Eq. (1) is three-body Green's function, Faddeev partition indices  $\alpha, \beta = 1, 2, 3$  simultaneously define a particle ( $\alpha$ ) and the remaining pair ( $\beta\gamma$ ),  $\alpha \neq \beta \neq \gamma$ . The operator  $T_\alpha(z)$  is a two-body  $T$  matrix describing interaction in the ( $\beta\gamma$ ) pair.

A separable potential  $V_\alpha$  leading to the separable  $T$  matrix,

$$V_\alpha = \lambda_\alpha |g_\alpha\rangle\langle g_\alpha| \rightarrow T_\alpha(z) = |g_\alpha\rangle\tau_\alpha(z)\langle g_\alpha|, \quad (2)$$

allows writing the three-body AGS equations in the form

$$X_{\alpha\beta}(z) = Z_{\alpha\beta}(z) + \sum_{\gamma=1}^3 Z_{\alpha\gamma}(z)\tau_\gamma(z)X_{\gamma\beta}(z), \quad (3)$$

with new transition  $X_{\alpha\beta}$  and kernel  $Z_{\alpha\beta}$  operators, defined by

$$X_{\alpha\beta}(z) = \langle g_\alpha | G_0(z) U_{\alpha\beta}(z) G_0(z) | g_\beta \rangle, \quad (4)$$

$$Z_{\alpha\beta}(z) = (1 - \delta_{\alpha\beta}) \langle g_\alpha | G_0(z) | g_\beta \rangle. \quad (5)$$

Here, for simplicity, the one-term separable potentials Eq. (2) is used, while in general  $V_\alpha$  can consist of  $N$  terms.

The four-body Faddeev-type Grassberger-Sandhas (GS) equations were derived in Ref. [16]:

$$U_{\alpha\beta}^{\sigma\rho}(z) = (1 - \delta_{\sigma\rho})\delta_{\alpha\beta}G_0^{-1}(z)T_\alpha^{-1}(z)G_0^{-1}(z) + \sum_{\tau,\gamma} (1 - \delta_{\sigma\tau})U_{\alpha\gamma}^\tau G_0(z)T_\gamma(z)G_0(z)U_{\gamma\beta}^{\tau\rho}. \quad (6)$$

In addition to the free Green's function  $G_0(z)$ , which now acts in four-body space, the two-body  $T$  matrix  $T_\alpha(z)$ , three-body  $U_{\alpha\beta}^\tau(z)$ , and four-body  $U_{\alpha\beta}^{\sigma\rho}(z)$  operators enter the system (6). The high indices  $\sigma, \rho, \tau$  define a partition, which could be 3 + 1 or 2 + 2 type, while the low indices  $\alpha, \beta$  define two-body subsystems of the particular three-body subsystem, denoted by the high index.

If the separable potentials (2), leading to the corresponding separable  $T$  matrices, are used, the system (6) can be rewritten in the same way as the three-body one. The new system of equations,

$$\begin{aligned} \bar{U}_{\alpha\beta}^{\sigma\rho}(z) &= (1 - \delta_{\sigma\rho})(\bar{G}_0^{-1})_{\alpha\beta}(z) \\ &+ \sum_{\tau,\gamma,\delta} (1 - \delta_{\sigma\tau})\bar{T}_{\alpha\gamma}^\tau(z)(\bar{G}_0)_{\gamma\delta}(z)\bar{U}_{\delta\beta}^{\tau\rho}(z), \end{aligned} \quad (7)$$

contains new operators

$$\bar{U}_{\alpha\beta}^{\sigma\rho}(z) = \langle g_\alpha | G_0(z) U_{\alpha\beta}^{\sigma\rho}(z) G_0(z) | g_\beta \rangle, \quad (8)$$

$$\bar{T}_{\alpha\beta}^\tau(z) = \langle g_\alpha | G_0(z) U_{\alpha\beta}^\tau(z) G_0(z) | g_\beta \rangle, \quad (9)$$

$$(\bar{G}_0)_{\alpha\beta}(z) = \delta_{\alpha\beta}\tau_\alpha(z). \quad (10)$$

It is seen that the four-body system with separable potentials Eq. (7) looks similarly to Eq. (1), which describes a three-body system with arbitrary potentials. This analogy can be used for further modification of the equations. Namely, if the three-body  $T$  matrices  $\bar{T}_{\alpha\beta}^\tau(z)$  in Eq. (7) are presented in a separable form

$$\bar{T}_{\alpha\beta}^\tau(z) = |\bar{g}_\alpha^\tau\rangle\bar{\tau}_{\alpha\beta}^\tau(z)\langle\bar{g}_\beta^\tau|, \quad (11)$$

the four-body equations Eq. (7) can be rewritten as [18]

$$\bar{X}_{\alpha\beta}^{\sigma\rho}(z) = \bar{Z}_{\alpha\beta}^{\sigma\rho}(z) + \sum_{\tau,\gamma,\delta} \bar{Z}_{\alpha\gamma}^{\sigma\tau}(z)\bar{\tau}_{\gamma\delta}^\tau(z)\bar{X}_{\delta\beta}^{\tau\rho}(z), \quad (12)$$

with new transition  $\bar{X}_{\alpha\beta}^{\sigma\rho}$  and kernel  $\bar{Z}_{\alpha\beta}^{\sigma\rho}$  operators, defined by

$$\bar{X}_{\alpha\beta}^{\sigma\rho}(z) = \langle \bar{g}_\alpha^\sigma | (\bar{G}_0)_{\alpha\alpha}(z) \bar{U}_{\alpha\beta}^{\sigma\rho}(z) (\bar{G}_0)_{\beta\beta}(z) | \bar{g}_\beta^\rho \rangle, \quad (13)$$

$$\bar{Z}_{\alpha\beta}^{\sigma\rho}(z) = (1 - \delta_{\sigma\rho}) \langle \bar{g}_\alpha^\sigma | (\bar{G}_0)_{\alpha\beta}(z) | \bar{g}_\beta^\rho \rangle. \quad (14)$$

In a general case, the separable three-body  $T$  matrices are represented by  $N$ -term operators, which enlarges the number of the coupled equations in the system Eq. (12).

The four-body equations Eq. (12) were solved in the present study with separable two-body  $T$  matrices being an input and three-body  $T$  matrices represented in a separable form.

## III. SEPARABLE THREE-BODY AMPLITUDES

The  $\bar{K}N$  and  $NN$  potentials, which were used in the present four-body calculations, are separable ones by construction. Therefore, separable versions of three-body and 2 + 2 amplitudes, entering the equations (12), should be constructed. These amplitudes are described by three-body AGS equations (3), being written in momentum basis for  $s$ -wave interactions have the form

$$\begin{aligned} X_{\alpha\beta}(p, p'; z) &= Z_{\alpha\beta}(p, p'; z) + \sum_{\gamma=1}^3 4\pi \int_0^\infty Z_{\alpha\gamma}(p, p''; z) \tau_\gamma \\ &\times (p''; z) X_{\gamma\beta}(p'', p'; z) p'^2 dp''. \end{aligned} \quad (15)$$

Here  $p, p'$ , and  $z$  are relative momenta and three-body energy. It is possible to evaluate eigenvalues  $\lambda_n$  and eigenfunctions  $g_{n\alpha}(p; z)$  of the system (15) from

$$\begin{aligned} g_{n\alpha}(p; z) &= \frac{1}{\lambda_n} \sum_{\gamma=1}^3 4\pi \int_0^\infty Z_{\alpha\gamma}(p, p'; z) \tau_\gamma(p'; z) g_{n\gamma} \\ &\times (p'; z) p'^2 dp', \end{aligned} \quad (16)$$

with normalization condition

$$\sum_{\gamma=1}^3 4\pi \int_0^\infty g_{n\gamma}(p'; z) \tau_\gamma(p'; z) g_{n'\gamma}(p'; z) p'^2 dp' = -\delta_{nn'}. \quad (17)$$

Knowledge of the eigenvalues and eigenfunction allows us to write down Hilbert-Schmidt expansion (HSE) of the kernel functions  $Z_{\alpha\beta}$ :

$$Z_{\alpha\beta}^{\text{HSE}}(p, p'; z) = - \sum_{n=1}^{\infty} \lambda_n g_{n\alpha}(p; z) g_{n\beta}(p'; z), \quad (18)$$

which leads to the separable three-body amplitude

$$X_{\alpha\beta}^{\text{HSE}}(p, p'; z) = - \sum_{n=1}^{\infty} \frac{\lambda_n}{1 - \lambda_n} g_{n\alpha}(p; z) g_{n\beta}(p'; z). \quad (19)$$

Since the kernel function  $Z_{\alpha\beta}$  and three-body amplitude  $X_{\alpha\beta}$  are energy-dependent functions, entering the four-body equations (12) off energy shell, it is necessary to solve eigenequations (16) with normalization condition (17) for every value of the three-body energy during the four-body calculations. Such a way of  $X_{\alpha\beta}^{\text{HSE}}(p, p'; z)$  calculation is time-consuming work. Due to this, the energy-dependent pole expansion or approximation (EDPE or EDPA) method, which was suggested in Ref. [19] specifically for the four-body Faddeev-type GS equations, was used in the previous study. EDPE needs a solution of the eigenequations (16) only once for a fixed energy  $z_{\text{fix}}$ . Usually it is chosen to be the binding energy  $z_{\text{fix}} = E_B$  if a bound state in the system exists or  $z_{\text{fix}} = 0$  if not. After that, energy-dependent form factors

$$g_{n\alpha}(p; z) = \sum_{\gamma=1}^3 4\pi \int_0^{\infty} Z_{\alpha\gamma}(p, p'; z) \tau_{\gamma}(p'; z_{\text{fix}}) g_{n\gamma} \times (p'; z_{\text{fix}}) p'^2 dp' \quad (20)$$

and propagators

$$[\Theta(z)]_{mn}^{-1} = \sum_{\gamma=1}^3 4\pi \int_0^{\infty} g_{m\gamma}(p'; z) \tau_{\gamma}(p'; z_{\text{fix}}) g_{n\gamma}(p'; z_{\text{fix}}) p'^2 dp' - \sum_{\gamma=1}^3 4\pi \int_0^{\infty} g_{m\gamma}(p'; z) \tau_{\gamma}(p'; z) g_{n\gamma}(p'; z) p'^2 dp' \quad (21)$$

are calculated. Finally, the separable three-body amplitude is written in the form

$$X_{\alpha\beta}^{\text{EDPE}}(p, p'; z) = \sum_{m,n=1}^{\infty} g_{m\alpha}(p; z) \Theta_{mn}(z) g_{n\beta}(p'; z). \quad (22)$$

If only one term is taken in the sums in Eq. (22), the energy-dependent pole expansion turns into the energy-dependent pole approximation. It is seen that the EDPE method needs only one solution of the eigenvalue equations (16) and calculations of the integrals (20) and (21) after that. According to the authors of the method [19], the series (22) converges faster than the Hilbert-Schmidt expansion, and the EDPE is accurate already with one term.

Three-body form factors  $g_{\alpha}$  in Eqs. (20)–(22) are denoted  $\bar{g}_{\alpha}^{\rho}$  in the four-body equations, while three-body energy-dependent functions  $\Theta(z)$  are denoted  $\bar{\tau}_{\alpha\beta}^{\rho}$  [four-body equations are written down for EDPA, i.e., only one term is taken in Eq. (22),  $m = n = 1$ ].

Different versions of numerical treatment of Eqs. (16) and (17) and Eqs. (20)–(22) were tried. The best results were obtained with the ZGEEV subroutine from Intel oneAPI Math Kernel Library - Fortran, which computes the eigenvalues and the left and/or right eigenvectors for an  $n$ -by- $n$  complex nonsymmetric matrix. The whole set of the eigenvalues and the corresponding eigenfunctions was evaluated. It means that the number of the calculated eigenvalues  $N_{\text{eig}}$  is equal to the number of the number  $N_{\text{int}}$  of points in sums, replacing the integrals in the eigenequation (16) and normalization condition (17), multiplied by the number of the equations in the system (15) ( $N_{\text{eig}}$  eigenfunctions for each of the  $N_{\text{eig}}$  eigenvalues). After that, the first term of the series in Eq. (22) with  $m = n = 1$  gives the correct binding energy [more exactly,  $\Theta_{11}(z) \xrightarrow{z \rightarrow E_B} \infty$ ] since the first eigenvalue was strictly set  $\lambda_1 = 1$  (of course when binding energy in the system exists).

The best approximation of the original kernel function  $Z_{\alpha\beta}(p, p'; z)$  is achieved when the number  $N_{\text{expt}}$  of terms in the series (22) is equal to the number  $N_{\text{int}}$  of integration points multiplied by the number of equations in Eq. (15). In this case the approximate value  $Z_{\alpha\beta}^{\text{EDPE}}(p, p'; z)$  coincides with the original one up to  $\approx 10$  significant digits. However, an increase of  $N_{\text{expt}}$  leads to a drastic growth in the number of coupled integral equations in the four-body system. On the other hand, an insufficient number of integration points  $N_{\text{int}}$  does not allow reproducing the binding energies in the system. Keeping all this in mind, the number of integration points  $N_{\text{int}}$ , which is enough for accurate calculations of the corresponding binding energy of the three-body subsystem, was used in the present study.

#### IV. FOUR-BODY EQUATIONS FOR THE $\bar{K}NNN$ SYSTEM

Two types of partitions of 3 + 1 and 2 + 2 type for the four-body  $\bar{K}NNN$  system are  $|\bar{K} + (NNN)\rangle$ ,  $|N + (\bar{K}NN)\rangle$ , and  $|(\bar{K}N) + (NN)\rangle$ . The present work started by writing down the system (12) for 18 channels considering three nucleons as nonidentical particles. Four-body asymptotic states are denoted by  $_{\alpha}^{\sigma}$  indices where  $\sigma = 1, 2, 3$  stands for  $|\bar{K} + (NNN)\rangle$ ,  $|N + (\bar{K}NN)\rangle$ , and  $|(\bar{K}N) + (NN)\rangle$  partitions, correspondingly, and  $\alpha = N_i N_j$  or  $\bar{K} N_i$  ( $i, j = 1, 2, 3, i \neq j$ ) denotes the pair in the two- or three-body subsystem:

$$\begin{aligned} \bar{g}_{N_i N_j}^1 &: |\bar{K} + (N_1 + N_2 N_3)\rangle, |\bar{K} + (N_2 + N_3 N_1)\rangle, |\bar{K} + (N_3 + N_1 N_2)\rangle, \\ \bar{g}_{N_i N_j}^2 &: |N_1 + (\bar{K} + N_2 N_3)\rangle, |N_2 + (\bar{K} + N_3 N_1)\rangle, |N_3 + (\bar{K} + N_1 N_2)\rangle, \\ \bar{g}_{\bar{K} N_i}^2 &: |N_1 + (N_2 + \bar{K} N_3)\rangle, |N_2 + (N_3 + \bar{K} N_1)\rangle, |N_3 + (N_1 + \bar{K} N_2)\rangle, \\ &|N_1 + (N_3 + \bar{K} N_2)\rangle, |N_2 + (N_1 + \bar{K} N_3)\rangle, |N_3 + (N_2 + \bar{K} N_1)\rangle, \\ \bar{g}_{N_i N_j}^3 &: |(N_2 N_3) + (\bar{K} + N_1)\rangle, |(N_3 N_1) + (\bar{K} + N_2)\rangle, |(N_1 N_2) + (\bar{K} + N_3)\rangle, \\ \bar{g}_{\bar{K} N_i}^3 &: |(\bar{K} N_1) + (N_2 + N_3)\rangle, |(\bar{K} N_2) + (N_3 + N_1)\rangle, |(\bar{K} N_3) + (N_1 + N_2)\rangle. \end{aligned} \quad (23)$$

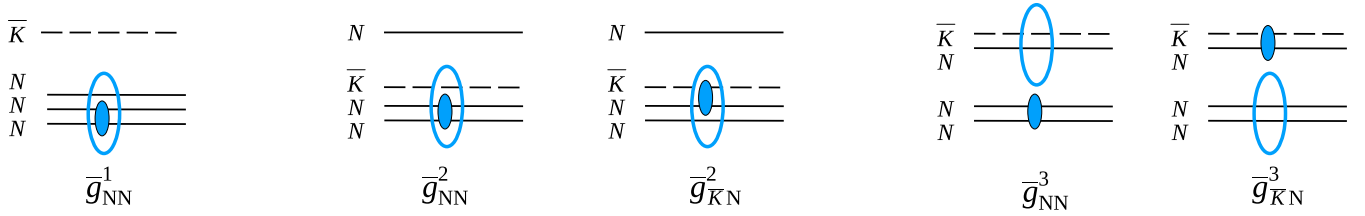


FIG. 1. States of the four-body system equations.

After antisymmetrization, necessary for a system with identical fermions, only five states, plotted in Fig. 1, remain. The kernel functions  $\bar{Z}_{\alpha}^{\sigma\rho}$  of the system of four-body equations (12) can be seen in Fig. 2 (where  $\bar{Z}_{\alpha\beta}^{\sigma\rho}$  carries only one bottom index due to  $\delta_{\alpha\beta}$  function in its definition).

Looking for a quasibound state requires solving the homogeneous system of equations, which can be written in a matrix form

$$\hat{X} = \hat{Z}\hat{t}\hat{X}, \quad (24)$$

with

$$\bar{X}_{\alpha}^{\rho} = \begin{pmatrix} \bar{X}_{NN}^1 \\ \bar{X}_{NN}^2 \\ \bar{X}_{KN}^2 \\ \bar{X}_{NN}^3 \\ \bar{X}_{KN}^3 \end{pmatrix}, \quad \bar{Z}_{\alpha}^{\sigma\rho} = \begin{pmatrix} 0 & \bar{Z}_{NN}^{12} & 0 & \bar{Z}_{NN}^{13} & 0 \\ \bar{Z}_{NN}^{21} & 0 & 0 & \bar{Z}_{NN}^{23} & 0 \\ 0 & 0 & \bar{Z}_{KN}^{22} & 0 & \bar{Z}_{KN}^{23} \\ \bar{Z}_{NN}^{31} & \bar{Z}_{NN}^{32} & 0 & 0 & 0 \\ 0 & 0 & \bar{Z}_{KN}^{32} & 0 & 0 \end{pmatrix}, \quad (25)$$

$$\bar{\tau}_{\alpha\beta}^{\rho} = \begin{pmatrix} \bar{\tau}_{NN,NN}^1 & 0 & 0 & 0 & 0 \\ 0 & \bar{\tau}_{NN,NN}^2 & \bar{\tau}_{NN,\bar{K}N}^2 & 0 & 0 \\ 0 & \bar{\tau}_{\bar{K}N,NN}^2 & \bar{\tau}_{\bar{K}N,\bar{K}N}^2 & 0 & 0 \\ 0 & 0 & 0 & \bar{\tau}_{NN,NN}^3 & \bar{\tau}_{NN,\bar{K}N}^3 \\ 0 & 0 & 0 & \bar{\tau}_{\bar{K}N,NN}^3 & \bar{\tau}_{\bar{K}N,\bar{K}N}^3 \end{pmatrix}. \quad (26)$$

However, our  $\bar{K}N$  and  $NN$  potentials, which were used for the  $\bar{K}NNN$  system calculations, are isospin- and spin-dependent interaction models. In addition,  $V_{NN}$  is a two-term potential. Due to this elements of the matrices  $\bar{Z}_{\alpha}^{\sigma\rho}$  in Eq. (25) and  $\bar{\tau}_{\alpha\beta}^{\rho}$  in Eq. (26), entering the antisymmetrized equations (24) are matrices themselves containing elements with additional indices  $\bar{Z}_{\alpha(m_2, n_2); (i, s, s')}^{\sigma\rho(m_3, n_3)}$  and  $\bar{\tau}_{\alpha\beta(m_2, m_2'); (i', s, s')}^{\rho(m_3)}$ . Here the indices  $m_3, n_3$  denote the number of a separable term of the three-body or  $2 + 2$  amplitudes (at the first step only one separable term was used for the three-body  $\bar{K}NN, NNN$  and  $2 + 2 \bar{K}N + NN$  amplitudes in Eq. (22), so that  $m_3 = n_3 = 1$ ). Separable indices  $m_2, n_2$  of the two-body subsystems (i.e., potentials) are  $m_2 = 1$  for  $V_{\bar{K}N}$  and  $m_2 = 1, 2$  for  $V_{NN}$ . The remaining indices  $i, i'$  and  $s, s'$  are two-body isospins and spins, correspondingly. Particular forms of nine matrices  $\bar{Z}_{\alpha}^{\sigma\rho}$  of Eq. (25) and nine matrices  $\bar{\tau}_{\alpha\beta}^{\rho}$  of Eq. (26) are presented in the Appendix.

The unknown four-body amplitudes in Eq. (25) have a general form  $\bar{X}_{\alpha\beta(m_2, n_2); (i, s, s')}^{\sigma\rho(m_3, n_3)}$ . Finally, the system to be solved, written in momentum representation, consists of 18 coupled integral equations.

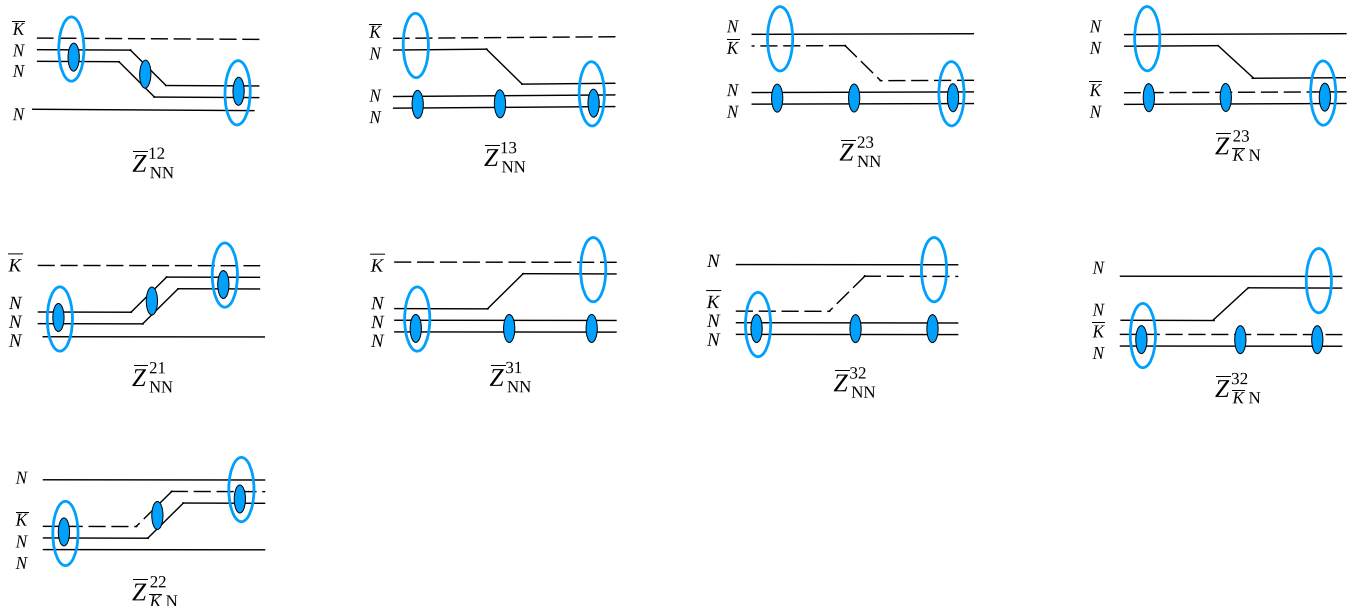


FIG. 2. Kernel functions  $\bar{Z}_{\alpha}^{\sigma\rho}$  of the four-body system equations.

## V. TWO-BODY INTERACTIONS AND THREE-BODY SUBSYSTEMS

### A. Two-body input: $\bar{K}N$ and $NN$ potentials

Both  $\bar{K}N$  and  $NN$  potentials, which were used, are separable isospin- and spin-dependent ones in  $s$  wave. Our three separable antikaon-nucleon potentials were constructed for our three-body calculations of the  $\bar{K}NN$  and  $\bar{K}\bar{K}N$  systems [10]. They are two phenomenological potentials with coupled  $\bar{K}N$ - $\pi\Sigma$  channels, having one-  $V_{\bar{K}N}^{1,SIDD}$  or two-pole  $V_{\bar{K}N}^{2,SIDD}$  structure of the  $\Lambda(1405)$  resonance [20] and a chirally motivated model  $V_{\bar{K}N}^{\text{Chiral}}$  with coupled  $\bar{K}N$ - $\pi\Sigma$ - $\pi\Lambda$  channels and the two-pole structure [21]. All three potentials reproduce low-energy  $K^-p$  scattering data, in particular elastic  $K^-p \rightarrow K^-p$  and inelastic  $K^-p \rightarrow \bar{K}^0n$ ,  $K^-p \rightarrow \pi^+\Sigma^-$ ,  $K^-p \rightarrow \pi^-\Sigma^+$ ,  $K^-p \rightarrow \pi^0\Sigma^0$ ,  $K^-p \rightarrow \pi^0\Lambda$  cross sections (the last one is reproduced only by the chirally motivated potential),

measured by several experiments [22–27]. The chirally motivated  $\bar{K}N$  potential also reproduces the medium values of three threshold branching ratios  $\gamma$ ,  $R_c$ ,  $R_n$  of the  $K^-p$  scattering:

$$\gamma = \frac{\Gamma(K^-p \rightarrow \pi^+\Sigma^-)}{\Gamma(K^-p \rightarrow \pi^-\Sigma^+)} = 2.36 \pm 0.04, \quad (27)$$

$$R_c = \frac{\Gamma(K^-p \rightarrow \pi^+\Sigma^-, \pi^-\Sigma^+)}{\Gamma(K^-p \rightarrow \text{all inelastic channels})} = 0.664 \pm 0.011, \quad (28)$$

$$R_n = \frac{\Gamma(K^-p \rightarrow \pi^0\Lambda)}{\Gamma(K^-p \rightarrow \text{neutral states})} = 0.189 \pm 0.015, \quad (29)$$

measured in Refs. [28,29]. The phenomenological  $\bar{K}N$  potentials take the lowest  $\pi\Lambda$  channel into account indirectly, through imaginary part of one of the strength constants. Due to this a new ratio

$$R_{\pi\Sigma} = \frac{\Gamma(K^-p \rightarrow \pi^+\Sigma^-) + \Gamma(K^-p \rightarrow \pi^-\Sigma^+)}{\Gamma(K^-p \rightarrow \pi^+\Sigma^-) + \Gamma(K^-p \rightarrow \pi^-\Sigma^+) + \Gamma(K^-p \rightarrow \pi^0\Sigma^0)}, \quad (30)$$

which contains the measured  $R_c$  and  $R_n$  and has an ‘‘experimental’’ value

$$R_{\pi\Sigma} = \frac{R_c}{1 - R_n(1 - R_c)} = 0.709 \pm 0.011, \quad (31)$$

was constructed. The medium value of this  $R_{\pi\Sigma}$  threshold branching ratio (31) together with the medium value of  $\gamma$  (27) is reproduced by both our phenomenological  $\bar{K}N$  potentials. All three of our antikaon-nucleon potentials also reproduce the  $1s$  level shift of kaonic hydrogen caused by the strong  $\bar{K}N$  interaction in comparison to the pure Coulomb level, measured by the SIDDHARTA experiment [30]:  $\Delta_{1s}^{SIDD} = -283 \pm 36 \pm 6$  eV, and its width  $\Gamma_{1s}^{SIDD} = 541 \pm 89 \pm 22$  eV. All the experimental data are described by our three potentials with equally high accuracy. In addition, elastic  $\pi\Sigma$  cross sections with isospin  $I_{\pi\Sigma} = 0$ , provided by all three potentials, have a bump in a region of the  $\Lambda(1405)$  resonance (according to PDG [31]:  $M_{\Lambda(1405)}^{PDG} = 1405.1_{-1.0}^{+1.3}$  MeV,  $\Gamma_{\Lambda(1405)}^{PDG} = 50.5 \pm 2.0$  MeV). The poles corresponding to the  $\Lambda(1405)$  resonance are situated at

$$z_{\Lambda(1405)-1}^{1,SIDD} = 1426 - i48\text{MeV}, \quad (32)$$

$$z_{\Lambda(1405)-1}^{2,SIDD} = 1414 - i58\text{MeV}, \quad z_{\Lambda(1405)-2}^{2,SIDD} = 1386 - i104\text{MeV}, \quad (33)$$

for the phenomenological potentials with one- and two-pole structure, correspondingly [21], and at

$$z_{\Lambda(1405)-1}^{\text{Chiral}} = 1417 - i33\text{MeV}, \quad z_{\Lambda(1405)-2}^{\text{Chiral}} = 1406 - i89\text{MeV}, \quad (34)$$

for the chirally motivated potential [32].

These phenomenological antikaon-nucleon potentials with coupled  $\bar{K}N$ - $\pi\Sigma$  channels were used in their original form in the three-body AGS equations [10] with coupled  $\bar{K}NN$ - $\pi\Sigma$  three-body channels. By this, the channel coupling was

taken into account directly. The chirally motivated potential, which additionally couples the  $\pi\Lambda$  channel, was used in a form of the two-channel exact optical  $\bar{K}N$ - $\pi\Sigma$ - $(-\pi\Lambda)$  potential. The four-body GS equations (12) are too complicated for introducing additional particle channels and performing coupled-channel calculations. Due to this the exact optical versions of our three  $\bar{K}N$  potentials [33], which are one-channel  $V_{\bar{K}N(-\pi\Sigma-\pi\Lambda)}$ , were used in the present study. They have exactly the same elastic part as the potential with coupled channels, while all inelasticity is taken into account in an energy-dependent imaginary part of the potential. It was demonstrated in our three-body calculations [33,34], that such exact optical potentials give quite accurate results for  $K^-d$  scattering length or quasibound-state position and width of the  $K^-pp$  system in comparison with the results obtained with the coupled-channel form. Due to this, it is assumed here that it could be a good approximation for the four-body calculations as well.

Nucleon-nucleon potentials  $V_{NN}^{\text{TSA-A}}$  and  $V_{NN}^{\text{TSA-B}}$  from our three-body calculations [10] were used here together with the new version of the two-term separable  $NN$  potential  $V_{NN}^{\text{TSN}}$ , described in Ref. [34]. All three potentials reproduce Argonne v18  $NN$  phase shifts at low energies up to 500 MeV with a change of sign, which means they are repulsive at short distances. They give proper singlet and triplet  $NN$  scattering lengths and deuteron binding energy. The new nucleon-nucleon potential  $V_{NN}^{\text{TSN}}$  reproduces Argonne v18  $pp$  phase shifts slightly better than the previously used ones, and its parameters are more natural than those of the older  $V_{NN}^{\text{TSA}}$  model.

In principle, Coulomb interaction also should be included in the equations, but the object of interest here is the quasibound state caused mainly by the strong potentials. The Coulomb interaction plays a minor role in such a state and can be neglected.

TABLE I. Dependence of the binding energy  $B_{K^-pp}^{\text{Opt}}$  (MeV) and width  $\Gamma_{K^-pp}^{\text{Opt}}$  (MeV) of the quasibound state in the  $K^-pp-\bar{K}^0np$  subsystem ( $\bar{K}NN$ ,  $S^{(3)} = 0$ ) on three  $\bar{K}N$  and three  $NN$  interaction models. Calculations were performed using the exact optical  $\bar{K}N$  potentials. The binding energy is counted from the threshold energy of the  $K^-pp$  system  $z_{th,K^-pp} = m_{\bar{K}} + 2m_N = 2373.485$  MeV.

	$V_{NN}^{\text{TSA-A}}$		$V_{NN}^{\text{TSA-B}}$		$V_{NN}^{\text{TSN}}$	
	$B_{K^-pp}^{\text{Opt}}$	$\Gamma_{K^-pp}^{\text{Opt}}$	$B_{K^-pp}^{\text{Opt}}$	$\Gamma_{K^-pp}^{\text{Opt}}$	$B_{K^-pp}^{\text{Opt}}$	$\Gamma_{K^-pp}^{\text{Opt}}$
$V_{\bar{K}N}^{1,\text{SIDD}}$	55.4	60.9	54.3	60.8	53.3	64.7
$V_{\bar{K}N}^{2,\text{SIDD}}$	48.2	46.2	47.5	45.9	46.7	48.4
$V_{\bar{K}N}^{\text{Chiral}}$	31.9	42.2	33.2	48.7	29.9	48.2

### B. 3 + 1 and 2 + 2 partitions

The  $\bar{K}NNN$  system with the lowest value of the four-body isospin  $I^{(4)} = 0$  and spin  $S^{(4)} = 1/2$ , which is  $K^-ppn-\bar{K}^0nnp$  in particle representation, was studied. All two-body interactions are  $s$ -wave ones, and the total angular momentum is zero. For the  $\bar{K}NNN$  system with these quantum numbers, the following three-body subsystems contribute

- (i)  $\bar{K}NN$  with isospin  $I^{(3)} = 1/2$  and spin  $S^{(3)} = 0$  ( $K^-pp$ ) or spin  $S^{(3)} = 1$  ( $K^-np$ );
- (ii)  $NNN$  with isospin  $I^{(3)} = 1/2$  and spin  $S^{(3)} = 1/2$  ( ${}^3\text{H}$  or  ${}^3\text{He}$ );

together with the 2 + 2 partition

- (iii)  $\bar{K}N + NN$  with isospin  $I^{(4)} = 0$  and spin  $S^{(4)} = 1/2$ .

The three-body  $\bar{K}NN$  system with different quantum numbers was studied in our previous works. In particular, quasibound state pole positions and widths in the  $K^-pp$  system ( $\bar{K}NN$  with isospin  $I^{(3)} = 1/2$  and spin  $S^{(3)} = 0$ ) were calculated in Ref. [32] with older  $V_{NN}^{\text{TSA-B}}$  nucleon-nucleon potential. Recently, the calculations were repeated with the new  $V_{NN}^{\text{TSN}}$  [34], the results of the calculations with coupled  $\bar{K}NN$  and  $\pi\Sigma N$  channels can be found in Table 4 of the paper. Since the four-body calculations were performed with the exact optical  $\bar{K}N$  potentials, the binding energies and widths of the three-body  $\bar{K}NN$  subsystem and of the  $\bar{K}N + NN$  partition also should be evaluated with the same versions of the antikaon-nucleon interaction models. Binding energies  $B_{K^-pp}^{\text{Opt}}$  and widths  $\Gamma_{K^-pp}^{\text{Opt}}$  calculated using the exact optical versions of the three antikaon-nucleon  $V_{\bar{K}N}^{1,\text{SIDD}}$ ,  $V_{\bar{K}N}^{2,\text{SIDD}}$ ,  $V_{\bar{K}N}^{\text{Chiral}}$  potentials and three nucleon-nucleon  $V_{NN}^{\text{TSA-A}}$ ,  $V_{NN}^{\text{TSA-B}}$ ,  $V_{NN}^{\text{TSN}}$  potentials are shown in Table I. It is seen that the new  $NN$  potential changed quasibound state positions in the  $K^-pp$  system by few MeV.

No quasibound states similar to that one in  $K^-pp$  were found in the  $K^-np$  system ( $\bar{K}NN$  with isospin  $I^{(3)} = 1/2$  and spin  $S^{(3)} = 1$ ) in our previous calculations [21]. However, new nucleon-nucleon potential  $V_{NN}^{\text{TSN}}$  changed the picture: the quasibound state caused purely by strong interactions can exist in the  $K^-np$  system [34] in addition to the kaonic deuterium, which is an atomic state mainly caused by the Coulomb interaction. The binding energies and widths of the “strong”

TABLE II. Dependence of the binding energy  $B_{K^-np}^{\text{Opt}}$  (MeV) and width  $\Gamma_{K^-np}^{\text{Opt}}$  (MeV) of the quasibound state in the  $K^-np-\bar{K}^0nn$  subsystem ( $\bar{K}NN$ ,  $S^{(3)} = 1$ ) on three  $\bar{K}N$  and three  $NN$  interaction models. Calculations were performed using the exact optical  $\bar{K}N$  potentials. The energy is counted from the  $K^-d$  threshold  $z_{th,K^-d} = m_{\bar{K}} + 2m_N + E_{\text{deu}} = 2371.26$  MeV.

	$V_{NN}^{\text{TSA-A}}$		$V_{NN}^{\text{TSA-B}}$		$V_{NN}^{\text{TSN}}$	
	$B_{K^-np}^{\text{Opt}}$	$\Gamma_{K^-np}^{\text{Opt}}$	$B_{K^-np}^{\text{Opt}}$	$\Gamma_{K^-np}^{\text{Opt}}$	$B_{K^-np}^{\text{Opt}}$	$\Gamma_{K^-np}^{\text{Opt}}$
$V_{\bar{K}N}^{1,\text{SIDD}}$	1.6	70.1	0.8	67.6	1.9	68.7
$V_{\bar{K}N}^{2,\text{SIDD}}$	5.2	63.7	5.0	61.4	5.6	62.7
$V_{\bar{K}N}^{\text{Chiral}}$	2.6	46.4	2.4	53.1	2.3	45.5

$K^-np$  state obtained in the coupled-channel  $\bar{K}NN-\pi\Sigma N$  calculations with the two-pole  $V_{\bar{K}N}^{2,\text{SIDD}}$  and  $V_{\bar{K}N}^{\text{Chiral}}$  models can be found in Table 3 of Ref. [34]. The binding energy of the state is so close to the  $K^-d$  threshold that the  $NN$  interaction, playing in the  $\bar{K}N$  system secondary role, can change predictions for the existence of the quasibound state caused by the strong interactions in the  $K^-np$  system. No quasibound state was found with the one-pole  $V_{\bar{K}N}^{1,\text{SIDD}}$  potential even together with the new nucleon-nucleon interaction model. However, when not the coupled-channel calculations are performed, but those with the exact optical  $\bar{K}N$  potential, the “strong” quasibound state is seen in the  $K^-np$  for all three antikaon-nucleon and all three nucleon-nucleon interaction models. The binding energies  $B_{K^-np}^{\text{Opt}}$  and width  $\Gamma_{K^-np}^{\text{Opt}}$  evaluated with the exact optical versions of the  $V_{\bar{K}N}^{1,\text{SIDD}}$ ,  $V_{\bar{K}N}^{2,\text{SIDD}}$ ,  $V_{\bar{K}N}^{\text{Chiral}}$  potentials and three nucleon-nucleon  $V_{NN}^{\text{TSA-A}}$ ,  $V_{NN}^{\text{TSA-B}}$ ,  $V_{NN}^{\text{TSN}}$  potentials can be seen in Table II. The “exact optical” results for the new  $V_{NN}^{\text{TSN}}$  potential presented in Table 3 of Ref. [34] and in Table II of the present paper are slightly different due to the smaller number of integration points used in the four-body calculations and, correspondingly, in its subsystems.

The binding energies and widths of the quasibound states of the  $\bar{K}NN$  systems with spin zero and one were calculated using the three-body AGS equations (3). Details of three-body calculations can be found in Refs. [33,35]. The codes for numerical solution of the three-body AGS equations for the  $\bar{K}NN$  systems were then modified to construct separable versions of the three-body amplitudes, as described in Sec. III.

The three-body AGS equations (3) were written and numerically solved for the three-nucleon system  $NNN$  with three  $NN$  potentials  $V_{NN}^{\text{TSA-A}}$ ,  $V_{NN}^{\text{TSA-B}}$ ,  $V_{NN}^{\text{TSN}}$  as an input. The calculated binding energies of the system are equal for both  ${}^3\text{H}$  and  ${}^3\text{He}$  nuclei since the Coulomb interaction was not taken into account. They are presented in Table III. The resulting energies are larger than known values for the binding energy of triton 8.4820 MeV and helium-3 7.7181 MeV nuclei. Such overestimation is typical for separable  $NN$  potentials. The numerical code was afterward changed for construction of a separable version of the  $NNN$  amplitude.

Finally, the partition of the 2 + 2 type  $\bar{K}N + NN$  is a system with two noninteracting pairs of particles. It is specific for the four-body Faddeev-type equations, and it is not

TABLE III. Dependence of the binding energy  $B_{NNN}$  (MeV) of the bound state in the  $NNN$  subsystem ( $S^{(3)} = 1/2$ ) on three  $NN$  models. The binding energy is counted from the threshold energy of the  $NNN$  system  $z_{th,NNN} = 3m_N = 2816.76$  MeV.

$V_{NN}^{\text{TSA-A}}$	$V_{NN}^{\text{TSA-B}}$	$V_{NN}^{\text{TSN}}$
9.03	9.04	9.52

a simple sum of two-body  $\bar{K}N$  and  $NN$  amplitudes. The  $\bar{K}N + NN$  partition is described by a three-body system of AGS equations (3), therefore, it is a “three-body” amplitude. Only  $\bar{K}N + NN$  partition with spin-one  $NN$  pair has a quasibound state, the binding energies and widths are shown in Table IV. The fixed energy  $z_{fix}$  for the  $2 + 2$  partition with spin-zero  $NN$  pair was set to zero. The separable version of the corresponding  $\bar{K}N + NN$  amplitude was constructed in a similar way as in the case of  $\bar{K}NN$  and  $NNN$  three-body subsystems.

## VI. RESULTS AND DISCUSSION

The four-body GS equations were solved for the  $K^-ppn-\bar{K}^0np$  system (24)–(26) with elements (A1)–(A18) using the antikaon-nucleon and nucleon-nucleon potentials described above. At the first step one separable term in separable representation of the three-body  $\bar{K}NN$ ,  $NNN$  and “three-body”  $\bar{K}N + NN$  amplitudes (22) was taken, therefore the EDPA method was used. The binding energies  $B_{K^-ppn}$  and widths  $\Gamma_{K^-ppn}$  of the  $\bar{K}NNN$  system evaluated using three exact optical versions of the antikaon-nucleon potentials and three nucleon-nucleon interaction models are presented in Table V.

It is seen that the binding energy  $B_{K^-ppn}$  and width  $\Gamma_{K^-ppn}$  of the four-body quasibound state strongly depend on the model of antikaon-nucleon interaction. It is a property of the three-body  $\bar{K}NN$  and  $\bar{K}\bar{K}N$  systems as well. Phenomenological  $\bar{K}N(-\pi\Sigma)$  potentials give comparable binding energies, while the chirally motivated potential led to much more shallow state. As for the width, the one-pole phenomenological  $V_{\bar{K}N}^{1,\text{SIDD}}$  potential give an  $\approx 11$  MeV larger value than the two-pole phenomenological  $V_{\bar{K}N}^{2,\text{SIDD}}$  interaction model. The width

TABLE IV. Dependence of the binding energy  $B_{K^-p+np}^{\text{Opt}}$  (MeV) and width  $\Gamma_{K^-p+np}^{\text{Opt}}$  (MeV) of the quasibound state in the  $K^-p + np$  partition ( $\bar{K}N + NN$ ,  $S^{(4)} = 1/2$ ) on three  $\bar{K}N$  and three  $NN$  interaction models. Calculations were performed using the exact optical  $\bar{K}N$  potentials. The binding energy is counted from the threshold energy of the  $K^-npp$  system  $z_{th,K^-npp} = m_{\bar{K}} + 3m_N = 3312.405$  MeV.

	$V_{NN}^{\text{TSA-A}}$		$V_{NN}^{\text{TSA-B}}$		$V_{NN}^{\text{TSN}}$	
	$B_{K^-p+np}^{\text{Opt}}$	$\Gamma_{K^-p+np}^{\text{Opt}}$	$B_{K^-p+np}^{\text{Opt}}$	$\Gamma_{K^-p+np}^{\text{Opt}}$	$B_{K^-p+np}^{\text{Opt}}$	$\Gamma_{K^-p+np}^{\text{Opt}}$
$V_{\bar{K}N}^{1,\text{SIDD}}$	20.0	83.6	19.1	81.1	20.3	82.2
$V_{\bar{K}N}^{2,\text{SIDD}}$	25.4	71.3	24.0	70.8	25.1	70.4
$V_{\bar{K}N}^{\text{Chiral}}$	18.8	54.5	20.9	58.5	17.9	53.7

TABLE V. Dependence of the binding energy  $B_{K^-ppn}$  (MeV) and width  $\Gamma_{K^-ppn}$  (MeV) of the quasibound state in the  $K^-ppn-\bar{K}^0np$  system on three  $\bar{K}N$  and three  $NN$  potentials.

	$V_{NN}^{\text{TSA-A}}$		$V_{NN}^{\text{TSA-B}}$		$V_{NN}^{\text{TSN}}$	Other results	
	$B_{K^-ppn}$	$\Gamma_{K^-ppn}$	$B_{K^-ppn}$	$\Gamma_{K^-ppn}$	$B_{K^-ppn}$	$\Gamma_{K^-ppn}$	
$V_{\bar{K}N}^{1,\text{SIDD}}$	52.0	50.4	50.3	49.6	51.2	50.8	
$V_{\bar{K}N}^{2,\text{SIDD}}$	47.0	39.6	46.4	38.2	46.4	39.9	
$V_{\bar{K}N}^{\text{Chiral}}$	32.6	39.7	34.5	50.9	30.5	42.8	
AY [1]							108.0 20.0
BGL [13]							29.3 32.9
OHHMH [14]							
$V_{\bar{K}N}^{\text{Kyoto-I}}$							45.3 25.5
$V_{\bar{K}N}^{\text{Kyoto-II}}$							49.7 69.4
$V_{\text{AY}}^{\bar{K}N}$							72.6 78.6
ME [15]							
$V_{\bar{K}N}^{1,\text{SIDD}}$							73.5 22.0
$V_{\bar{K}N}^{2,\text{SIDD}}$							58.5 27.0
$V_{\bar{K}N}^{\text{IKS chiral}}$							41.4 31.5

of the quasibound state evaluated with the chirally motivated potential  $V_{\bar{K}N}^{\text{Chiral}}$  strongly depends on the nucleon-nucleon potential, the  $\Gamma_{K^-ppn}$  calculated with different  $V_{NN}$  vary by up to 11 MeV. Dependence of the corresponding “chiral” binding energies on the nucleon-nucleon interaction models is weaker. The characteristics of the  $K^-ppn$  state calculated with the phenomenological  $\bar{K}N$  potentials slightly depend on the  $V_{NN}$  potential.

Comparing the four-body binding energies and widths in Table V with those obtained for the three-body spin-zero  $\bar{K}NN$  system usually denoted as  $K^-pp$  (Table I), it is seen that the binding energies remain almost the same or become slightly smaller after adding one neutron, while the widths become much smaller. So that addition of the neutron to the  $K^-pp$  system changes the binding energy of the resulting system slightly, but it “tightens” the quasibound state.

On the other hand, the four-body  $K^-ppn$  binding energies are much larger than those for the spin-one  $K^-np$  state. The reason might be the additional strong  $K^-p$  attraction introduced by the extra for the  $K^-np$  system proton.

Very preliminary results of the present calculations, namely, the pole positions of the quasibound state in the  $K^-ppn-\bar{K}^0np$  system obtained with two phenomenological potentials were published in Ref. [[17,18,36]]. They differ from those presented in Table V drastically: binding energies are much larger while the widths are smaller. One of the reasons is the different numerical treatment of the separable representation of the three-body and “three-body” amplitudes. In contrast to the present usage of the Intel MKL library subroutine, some handmade subroutine for evaluation of eigenvalues and eigenfunctions were used in Ref. [36].

Results for the binding energies and widths by other authors are also presented in Table V. The largest binding energy and smaller width were predicted in Ref. [1] by Akaishi and Yamazaki using many-body  $G$ -matrix formalism for the few-body system and an antikaon-nucleon model, which does not

reproduce actual experimental data on  $K^-p$  scattering and kaonic hydrogen.

Barnea, Gal, and Liverts performed variational calculation [13] using an energy-dependent chiral  $\bar{K}N$  potential, which, however, was calculated at a set of fixed energies. The imaginary part of the quasibound state was also calculated approximately. The binding energy obtained in Ref. [13] is not far from the binding energy evaluated in the present calculations with our chirally motivated antikaon-nucleon potential, taken into account exactly. The width in Ref. [13], however, is much smaller.

Variational calculations also were performed by Ohnishi *et al.* in Ref. [14] with energy-dependent Kyoto and energy-independent AY  $\bar{K}N$  potentials. The authors also had to fix the antikaon-nucleon energy in the Kyoto potential, and they did it in two ways, denoting the corresponding models as Kyoto-I and Kyoto-II. A huge difference between the widths obtained with these two Kyoto potentials shows that the chosen procedure is not reliable. Besides, the binding energy and width of the four-body quasibound state, calculated in Ref. [14] with the AY potential, differs drastically from the original AY results [1].

The most intriguing is the difference between the present results and those of Ref. [15] by Marri and Esmaili since the authors solved the same four-body Faddeev-type equations, moreover, they used our phenomenological  $V_{\bar{K}N}^{1,\text{SIDD}}$  and  $V_{\bar{K}N}^{2,\text{SIDD}}$  potentials. Nucleon-nucleon PEST  $V_{NN}$  potential, which is a separable version of the Paris nucleon-nucleon interaction model was used there. But different  $NN$  potentials hardly could be responsible for such a drastic discrepancy of the results, by  $\approx 20$  MeV for both: binding energy (make it much larger) and width (make it much smaller).

One of the possible reasons for the differences could follow from the way the separable versions of the three-body and  $2+2$  amplitudes were constructed. The formulas for the EDPE energy-dependent form factors and propagators in Ref. [15] differ from those in Eqs. (20) and (21) by a factor  $1/\lambda$  on the right-hand side for the first and by  $m \leftrightarrow n$  in the second formula. Besides, setting the fixed energy for the  $(\bar{K}N)_{I=0} + NN$  to the binding energy of the quasibound  $\bar{K}N$  state [which is a  $\Lambda(1405)$  resonance], made by Marri and Esmaili in Ref. [15], is not quite understandable. The matter is the total four-body isospin  $I^{(4)} = 0$  means that the  $NN$  subsystem should also have  $I_{NN} = 0$ , which is a deuteron. Due to this, the total binding energy of this partition should include both two-body energies:  $B_{\Lambda(1405)}$  and  $B_{\text{deu}}$ . In fact, the energy of the  $\bar{K}N + NN$  “three-body” system with isospins of both pairs equal to zero differs from a simple sum of the two two-body energies, see Table IV. It comes from the solution of the three-body equation. As for another state of the  $\bar{K}N + NN$  partition, it does not have bound states since  $\bar{K}N$  and  $NN$  in this case have two-body isospin  $I^{(2)} = 1$  and none of them is bound. Setting the fixed energy in this case to the deuteron binding energy, as is done in Ref. [15], is quite strange.

Finally, the binding energy of the three-body  $K^-pp$  subsystem evaluated by Marri and Esmaili in Ref. [15] with our phenomenological  $V_{\bar{K}N}^{1,\text{SIDD}}$  potential differ from our three-body results by  $\approx 6$  MeV and almost coincides with the

binding energy calculated in Ref. [15] with  $V_{\bar{K}N}^{2,\text{SIDD}}$ . On the contrary, the three-body binding energies in Table I obtained with  $V_{\bar{K}N}^{1,\text{SIDD}}$  and  $V_{\bar{K}N}^{2,\text{SIDD}}$  differ one from another for each of the three nucleon-nucleon potentials. Keeping the closeness of the  $K^-pp$  three-body binding energies of Ref. [15] in mind, it is hard to understand the large difference (15 MeV) between the corresponding four-body  $K^-ppn$  results obtained in the same paper.

## VII. CONCLUSION

The four-body Faddeev-type GS equations for the search of the quasibound state in the  $\bar{K}NNN$  system caused by strong interactions were written down and solved. The binding energies  $B_{K^-ppn}^{\text{Chiral}} \approx 30.5\text{--}34.5$  MeV obtained with chirally motivated and  $B_{K^-ppn}^{\text{SIDD}} \approx 46.4\text{--}52.0$  MeV obtained with phenomenological antikaon-nucleon potentials are close to those for the  $K^-pp$  system, calculated with the same  $V_{\bar{K}N}$  and  $V_{NN}$  potentials. The widths of the four-body states  $\Gamma_{K^-ppn} \approx 38.2\text{--}50.9$  MeV are smaller than the three-body widths of  $K^-pp$ . Therefore, the neutron added to the  $K^-pp$  system slightly influences the binding, but tightens the system.

The four-body binding energy and width of the  $K^-ppn$  system strongly depend on  $\bar{K}N$  potential. The results also noticeably depend on the nucleon-nucleon interaction model, when the chirally motivated antikaon-nucleon potential is used.

## ACKNOWLEDGMENT

The work was supported by GACR Grant No. 19-19640S.

## APPENDIX: ELEMENTS OF $\bar{Z}_{\alpha}^{\sigma\rho}$ AND $\bar{\tau}_{\alpha\beta}^{\rho}$ MATRICES

After antisymmetrization, the system (24) consists of 18 coupled equations. Elements of the matrices  $\bar{Z}_{\alpha}^{\sigma\rho}$  in Eq. (25) and  $\bar{\tau}_{\alpha\beta}^{\rho}$  in Eq. (26) are matrices themselves with elements  $\bar{Z}_{\alpha}^{\sigma\rho(m_3, n_3)}_{(i, s, i', s')}$  and  $\bar{\tau}_{\alpha\beta}^{\rho(m_2, m_2')}_{(i', s, i', s')}$ . Indices  $m_3, n_3$  denote the number of separable terms of the three-body or  $2+2$  amplitudes ( $m_3 = n_3 = 1$ ), while  $m_2, n_2$  are separable indices of the potentials:  $m_2 = 1$  for  $V_{\bar{K}N}$  and  $m_2 = 1, 2$  for  $V_{NN}$ . Two-body isospins and spins are denoted  $i, i'$  and  $s, s'$ , correspondingly.

The kernel matrices  $\bar{Z}_{\alpha}^{\sigma\rho}$  consist of six elements with  $\alpha = NN$ :

$$\bar{Z}_{NN}^{12} = \begin{pmatrix} \bar{Z}_{NN(1,1);(0,11)}^{12(1,1)} & 0 & \bar{Z}_{NN(1,2);(0,11)}^{12(1,1)} & 0 \\ 0 & \bar{Z}_{NN(1,1);(1,00)}^{12(1,1)} & 0 & \bar{Z}_{NN(1,2);(1,00)}^{12(1,1)} \\ \bar{Z}_{NN(2,1);(0,11)}^{12(1,1)} & 0 & \bar{Z}_{NN(2,2);(0,11)}^{12(1,1)} & 0 \\ 0 & \bar{Z}_{NN(2,1);(1,00)}^{12(1,1)} & 0 & \bar{Z}_{NN(2,2);(1,00)}^{12(1,1)} \end{pmatrix}, \quad (\text{A1})$$

$$\bar{Z}_{NN}^{13} = \begin{pmatrix} \bar{Z}_{NN(1,1);(0,11)}^{13(1,1)} & 0 & \bar{Z}_{NN(1,2);(0,11)}^{13(1,1)} & 0 \\ 0 & \bar{Z}_{NN(1,1);(1,00)}^{13(1,1)} & 0 & \bar{Z}_{NN(1,2);(1,00)}^{13(1,1)} \\ \bar{Z}_{NN(2,1);(0,11)}^{13(1,1)} & 0 & \bar{Z}_{NN(2,2);(0,11)}^{13(1,1)} & 0 \\ 0 & \bar{Z}_{NN(2,1);(1,00)}^{13(1,1)} & 0 & \bar{Z}_{NN(2,2);(1,00)}^{13(1,1)} \end{pmatrix}, \quad (\text{A2})$$



$$\bar{Z}_{NN}^{21} = \begin{pmatrix} \bar{Z}_{NN(1,1);(0,11)}^{21(1,1)} & 0 & \bar{Z}_{NN(1,2);(0,11)}^{21(1,1)} & 0 \\ 0 & \bar{Z}_{NN(1,1);(1,00)}^{21(1,1)} & 0 & \bar{Z}_{NN(1,2);(1,00)}^{21(1,1)} \\ \bar{Z}_{NN(2,1);(0,11)}^{21(1,1)} & 0 & \bar{Z}_{NN(2,2);(0,11)}^{21(1,1)} & 0 \\ 0 & \bar{Z}_{NN(2,1);(1,00)}^{21(1,1)} & 0 & \bar{Z}_{NN(2,2);(1,00)}^{21(1,1)} \end{pmatrix}, \quad (\text{A3})$$

$$\bar{Z}_{NN}^{23} = \begin{pmatrix} \bar{Z}_{NN(1,1);(0,11)}^{23(1,1)} & 0 & \bar{Z}_{NN(1,2);(0,11)}^{23(1,1)} & 0 \\ 0 & \bar{Z}_{NN(1,1);(1,00)}^{23(1,1)} & 0 & \bar{Z}_{NN(1,2);(1,00)}^{23(1,1)} \\ \bar{Z}_{NN(2,1);(0,11)}^{23(1,1)} & 0 & \bar{Z}_{NN(2,2);(0,11)}^{23(1,1)} & 0 \\ 0 & \bar{Z}_{NN(2,1);(1,00)}^{23(1,1)} & 0 & \bar{Z}_{NN(2,2);(1,00)}^{23(1,1)} \end{pmatrix}, \quad (\text{A4})$$

$$\bar{Z}_{NN}^{31} = \begin{pmatrix} \bar{Z}_{NN(1,1);(0,11)}^{31(1,1)} & 0 & \bar{Z}_{NN(1,2);(0,11)}^{31(1,1)} & 0 \\ 0 & \bar{Z}_{NN(1,1);(1,00)}^{31(1,1)} & 0 & \bar{Z}_{NN(1,2);(1,00)}^{31(1,1)} \\ \bar{Z}_{NN(2,1);(0,11)}^{31(1,1)} & 0 & \bar{Z}_{NN(2,2);(0,11)}^{31(1,1)} & 0 \\ 0 & \bar{Z}_{NN(2,1);(1,00)}^{31(1,1)} & 0 & \bar{Z}_{NN(2,2);(1,00)}^{31(1,1)} \end{pmatrix}, \quad (\text{A5})$$

$$\bar{Z}_{NN}^{32} = \begin{pmatrix} \bar{Z}_{NN(1,1);(0,11)}^{32(1,1)} & 0 & \bar{Z}_{NN(1,2);(0,11)}^{32(1,1)} & 0 \\ 0 & \bar{Z}_{NN(1,1);(1,00)}^{32(1,1)} & 0 & \bar{Z}_{NN(1,2);(1,00)}^{32(1,1)} \\ \bar{Z}_{NN(2,1);(0,11)}^{32(1,1)} & 0 & \bar{Z}_{NN(2,2);(0,11)}^{32(1,1)} & 0 \\ 0 & \bar{Z}_{NN(2,1);(1,00)}^{32(1,1)} & 0 & \bar{Z}_{NN(2,2);(1,00)}^{32(1,1)} \end{pmatrix}, \quad (\text{A6})$$

and three elements with  $\alpha = \bar{K}N$ ,

$$\bar{Z}_{\bar{K}N}^{22} = \begin{pmatrix} \bar{Z}_{\bar{K}N(1,1);(0,00)}^{22(1,1)} & 0 & \bar{Z}_{\bar{K}N(1,1);(0,01)}^{22(1,1)} & 0 \\ 0 & \bar{Z}_{\bar{K}N(1,1);(1,00)}^{22(1,1)} & 0 & \bar{Z}_{\bar{K}N(1,1);(1,01)}^{22(1,1)} \\ \bar{Z}_{\bar{K}N(1,1);(0,10)}^{22(1,1)} & 0 & \bar{Z}_{\bar{K}N(1,1);(0,11)}^{22(1,1)} & 0 \\ 0 & \bar{Z}_{\bar{K}N(1,1);(1,10)}^{22(1,1)} & 0 & \bar{Z}_{\bar{K}N(1,1);(1,11)}^{22(1,1)} \end{pmatrix}, \quad (\text{A7})$$

$$\bar{Z}_{\bar{K}N}^{23} = \begin{pmatrix} \bar{Z}_{\bar{K}N(1,1);(0,01)}^{23(1,1)} & 0 \\ 0 & \bar{Z}_{\bar{K}N(1,1);(1,00)}^{23(1,1)} \\ \bar{Z}_{\bar{K}N(1,1);(0,11)}^{23(1,1)} & 0 \\ 0 & \bar{Z}_{\bar{K}N(1,1);(1,10)}^{23(1,1)} \end{pmatrix}, \quad (\text{A8})$$

$$\bar{Z}_{\bar{K}N}^{32} = \begin{pmatrix} \bar{Z}_{\bar{K}N(1,1);(0,10)}^{32(1,1)} & 0 & \bar{Z}_{\bar{K}N(1,1);(0,11)}^{32(1,1)} & 0 \\ 0 & \bar{Z}_{\bar{K}N(1,1);(1,00)}^{32(1,1)} & 0 & \bar{Z}_{\bar{K}N(1,1);(1,01)}^{32(1,1)} \end{pmatrix}. \quad (\text{A9})$$

Elements of  $\bar{\tau}_{\alpha\beta}^{\rho}$  matrix (26) are parts of the  $NNN$  subsystem ( $\rho = 1$ ):

$$\bar{\tau}_{NN,NN}^1 = \begin{pmatrix} \bar{\tau}_{NN,NN(1,1);(0,011)}^1(1) & \bar{\tau}_{NN,NN(1,1);(0,10)}^1(1) & \bar{\tau}_{NN,NN(1,2);(0,011)}^1(1) & \bar{\tau}_{NN,NN(1,2);(0,10)}^1(1) \\ \bar{\tau}_{NN,NN(1,1);(1,001)}^1(1) & \bar{\tau}_{NN,NN(1,1);(1,00)}^1(1) & \bar{\tau}_{NN,NN(1,2);(1,001)}^1(1) & \bar{\tau}_{NN,NN(1,2);(1,00)}^1(1) \\ \bar{\tau}_{NN,NN(2,1);(0,011)}^1(1) & \bar{\tau}_{NN,NN(2,1);(0,10)}^1(1) & \bar{\tau}_{NN,NN(2,2);(0,011)}^1(1) & \bar{\tau}_{NN,NN(2,2);(0,10)}^1(1) \\ \bar{\tau}_{NN,NN(2,1);(1,001)}^1(1) & \bar{\tau}_{NN,NN(2,1);(1,00)}^1(1) & \bar{\tau}_{NN,NN(2,2);(1,001)}^1(1) & \bar{\tau}_{NN,NN(2,2);(1,00)}^1(1) \end{pmatrix}, \quad (\text{A10})$$

of the  $\bar{K}NN$  subsystem ( $\rho = 2$ ):

$$\bar{\tau}_{NN,NN}^2 = \begin{pmatrix} \bar{\tau}_{NN,NN(1,1);(00,11)}^{2(1)} & 0 & \bar{\tau}_{NN,NN(1,2);(00,11)}^{2(1)} & 0 \\ 0 & \bar{\tau}_{NN,NN(1,1);(11,00)}^{2(1)} & 0 & \bar{\tau}_{NN,NN(1,2);(11,00)}^{2(1)} \\ \bar{\tau}_{NN,NN(2,1);(00,11)}^{2(1)} & 0 & \bar{\tau}_{NN,NN(2,2);(00,11)}^{2(1)} & 0 \\ 0 & \bar{\tau}_{NN,NN(2,1);(11,00)}^{2(1)} & 0 & \bar{\tau}_{NN,NN(2,2);(11,00)}^{2(1)} \end{pmatrix}, \quad (\text{A11})$$

$$\bar{\tau}_{NN,\bar{K}N}^2 = \begin{pmatrix} 0 & 0 & \bar{\tau}_{NN,\bar{K}N(1,1);(00,11)}^{2(1)} & \bar{\tau}_{NN,\bar{K}N(1,1);(01,11)}^{2(1)} \\ \bar{\tau}_{NN,\bar{K}N(1,1);(10,00)}^{2(1)} & \bar{\tau}_{NN,\bar{K}N(1,1);(11,00)}^{2(1)} & 0 & 0 \\ 0 & 0 & \bar{\tau}_{NN,\bar{K}N(2,1);(00,11)}^{2(1)} & \bar{\tau}_{NN,\bar{K}N(2,1);(01,11)}^{2(1)} \\ \bar{\tau}_{NN,\bar{K}N(2,1);(10,00)}^{2(1)} & \bar{\tau}_{NN,\bar{K}N(2,1);(11,00)}^{2(1)} & 0 & 0 \end{pmatrix}, \quad (\text{A12})$$

$$\bar{\tau}_{\bar{K}N,NN}^2 = \begin{pmatrix} 0 & \bar{\tau}_{\bar{K}N,NN(1,1);(01,00)}^{2(1)} & 0 & \bar{\tau}_{\bar{K}N,NN(1,2);(01,00)}^{2(1)} \\ 0 & \bar{\tau}_{\bar{K}N,NN(1,1);(11,00)}^{2(1)} & 0 & \bar{\tau}_{\bar{K}N,NN(1,2);(11,00)}^{2(1)} \\ \bar{\tau}_{\bar{K}N,NN(1,1);(00,11)}^{2(1)} & 0 & \bar{\tau}_{\bar{K}N,NN(1,2);(00,11)}^{2(1)} & 0 \\ \bar{\tau}_{\bar{K}N,NN(1,1);(10,11)}^{2(1)} & 0 & \bar{\tau}_{\bar{K}N,NN(1,2);(10,11)}^{2(1)} & 0 \end{pmatrix}, \quad (\text{A13})$$

$$\bar{\tau}_{\bar{K}N,\bar{K}N}^2 = \begin{pmatrix} \bar{\tau}_{\bar{K}N,\bar{K}N(1,1);(00,00)}^{2(1)} & \bar{\tau}_{\bar{K}N,\bar{K}N(1,1);(01,00)}^{2(1)} & 0 & 0 \\ \bar{\tau}_{\bar{K}N,\bar{K}N(1,1);(10,00)}^{2(1)} & \bar{\tau}_{\bar{K}N,\bar{K}N(1,1);(11,00)}^{2(1)} & 0 & 0 \\ 0 & 0 & \bar{\tau}_{\bar{K}N,\bar{K}N(1,1);(00,11)}^{2(1)} & \bar{\tau}_{\bar{K}N,\bar{K}N(1,1);(01,11)}^{2(1)} \\ 0 & 0 & \bar{\tau}_{\bar{K}N,\bar{K}N(1,1);(10,11)}^{2(1)} & \bar{\tau}_{\bar{K}N,\bar{K}N(1,1);(11,11)}^{2(1)} \end{pmatrix}, \quad (\text{A14})$$

and of the  $\bar{K}N + NN$  partition ( $\rho = 3$ ):

$$\bar{\tau}_{NN,NN}^3 = \begin{pmatrix} \bar{\tau}_{NN,NN(1,1);(00,11)}^{3(1)} & 0 & \bar{\tau}_{NN,NN(1,2);(00,11)}^{3(1)} & 0 \\ 0 & \bar{\tau}_{NN,NN(1,1);(11,00)}^{3(1)} & 0 & \bar{\tau}_{NN,NN(1,2);(11,00)}^{3(1)} \\ \bar{\tau}_{NN,NN(2,1);(00,11)}^{3(1)} & 0 & \bar{\tau}_{NN,NN(2,2);(00,11)}^{3(1)} & 0 \\ 0 & \bar{\tau}_{NN,NN(2,1);(11,00)}^{3(1)} & 0 & \bar{\tau}_{NN,NN(2,2);(11,00)}^{3(1)} \end{pmatrix}, \quad (\text{A15})$$

$$\bar{\tau}_{NN,\bar{K}N}^3 = \begin{pmatrix} \bar{\tau}_{NN,\bar{K}N(1,1);(00,11)}^{3(1)} & 0 \\ 0 & \bar{\tau}_{NN,\bar{K}N(1,1);(11,00)}^{3(1)} \\ \bar{\tau}_{NN,\bar{K}N(2,1);(00,11)}^{3(1)} & 0 \\ 0 & \bar{\tau}_{NN,\bar{K}N(2,1);(11,00)}^{3(1)} \end{pmatrix}, \quad (\text{A16})$$

$$\bar{\tau}_{\bar{K}N,NN}^3 = \begin{pmatrix} \bar{\tau}_{\bar{K}N,NN(1,1);(00,11)}^{3(1)} & 0 & \bar{\tau}_{\bar{K}N,NN(1,2);(00,11)}^{3(1)} & 0 \\ 0 & \bar{\tau}_{\bar{K}N,NN(1,1);(11,00)}^{3(1)} & 0 & \bar{\tau}_{\bar{K}N,NN(1,2);(11,00)}^{3(1)} \end{pmatrix}, \quad (\text{A17})$$

$$\bar{\tau}_{\bar{K}N,\bar{K}N}^3 = \begin{pmatrix} \bar{\tau}_{\bar{K}N,\bar{K}N(1,1);(00,11)}^{3(1)} & 0 \\ 0 & \bar{\tau}_{\bar{K}N,\bar{K}N(1,1);(11,00)}^{3(1)} \end{pmatrix}. \quad (\text{A18})$$

- [1] Y. Akaishi and T. Yamazaki, *Phys. Rev. C* **65**, 044005 (2002).
- [2] T. Yamazaki and Y. Akaishi, *Phys. Lett. B* **535**, 70 (2002).
- [3] M. Agnello *et al.*, *Phys. Rev. Lett.* **94**, 212303 (2005).
- [4] T. Yamazaki *et al.*, *Phys. Rev. Lett.* **104**, 132502 (2010).
- [5] Y. Ichikawa *et al.*, *Prog. Theor. Exp. Phys.* **2015**, 21D01 (2015).
- [6] G. Agakishiev *et al.*, *Phys. Lett. B* **742**, 242 (2015).
- [7] O. Vazquez Doce *et al.*, *Phys. Lett. B* **758**, 134 (2016).
- [8] S. Ajimura *et al.* (J-PARK E15 Collaboration), *Phys. Lett. B* **789**, 620 (2019).
- [9] T. Yamaga *et al.* (J-PARK E15 Collaboration), *Phys. Rev. C* **102**, 044002 (2020).
- [10] N. V. Shevchenko, *Few-Body Syst.* **58**, 6 (2017).
- [11] T. Hashimoto *et al.* (J-PARK E62 Collaboration), *Phys. Rev. Lett.* **128**, 112503 (2022).
- [12] F. Sakuma *et al.* (J-PARK E80 Collaboration), proposal (unpublished).
- [13] N. Barnea, A. Gal, and E. Z. Liverts, *Phys. Lett. B* **712**, 132 (2012).
- [14] S. Ohnishi, W. Horiuchi, T. Hoshino, K. Miyahara, and T. Hyodo, *Phys. Rev. C* **95**, 065202 (2017).
- [15] S. Marri and J. Esmaili, *Eur. Phys. J. A* **55**, 43 (2019).
- [16] P. Grassberger and W. Sandhas, *Nucl. Phys. B* **2**, 181 (1967).
- [17] E. O. Alt, P. Grassberger, and W. Sandhas, *Nucl. Phys. B* **2**, 167 (1967).
- [18] A. Casel, H. Haberzettl, and W. Sandhas, *Phys. Rev. C* **25**, 1738 (1982).
- [19] S. Sofianos, N. J. McGurk, and H. Fiedeldeldey, *Nucl. Phys. A* **318**, 295 (1979).
- [20] N. V. Shevchenko, *Nucl. Phys. A* **890-891**, 50 (2012).
- [21] N. V. Shevchenko and J. Révai, *Phys. Rev. C* **90**, 034003 (2014).
- [22] M. Sakitt *et al.*, *Phys. Rev.* **139**, B719 (1965).
- [23] J. K. Kim, *Phys. Rev. Lett.* **14**, 29 (1965).
- [24] J. K. Kim, *Phys. Rev. Lett.* **19**, 1074 (1967).
- [25] W. Kittel, G. Otter, and I. Wacek, *Phys. Lett.* **21**, 349 (1966).
- [26] J. Ciborowski *et al.*, *J. Phys. G: Nucl. Phys.* **8**, 13 (1982).
- [27] D. Evans *et al.*, *J. Phys. G: Nucl. Phys.* **9**, 885 (1983).
- [28] D. N. Tovee, *Nucl. Phys. B* **33**, 493 (1971).
- [29] R. J. Nowak *et al.*, *Nucl. Phys. B* **139**, 61 (1978).
- [30] M. Bazzi *et al.* (SIDDHARTA Collaboration), *Phys. Lett. B* **704**, 113 (2011).
- [31] M. Tanabashi *et al.* (Particle Data Group), *Phys. Rev. D* **98**, 030001 (2018).
- [32] J. Révai and N. V. Shevchenko, *Phys. Rev. C* **90**, 034004 (2014).
- [33] N. V. Shevchenko, *Phys. Rev. C* **85**, 034001 (2012).
- [34] N. V. Shevchenko, *Few-Body Syst.* **61**, 27 (2020).
- [35] N. V. Shevchenko, A. Gal, J. Mares, and J. Revai, *Phys. Rev. C* **76**, 044004 (2007).
- [36] N. V. Shevchenko, *Sci. Post Phys. Proc.* **3**, 041 (2020).